

A WIDEBAND PLANAR MONOPOLE ANTENNA ARRAY WITH CIRCULAR POLARIZED AND BAND-NOTCHED CHARACTERISTICS

W.-S. Lee, K.-S. Oh^{*}, and J.-W. Yu

Department of Electrical Engineering, KAIST, 291 Daehak-ro, Yuseong-gu, Daejeon 305-701, Korea

Abstract—A wideband circular polarized planar monopole antenna array (PMAA) that employs dual band-notched characteristics is presented in this paper. The proposed antenna array is formed by four pinwheel-shaped folded planar monopole antennas (PMAs) in order to improve the performance of circular polarization and high directivity. Also, it achieves low-profile, small-sized structure. The attractive characteristics of the proposed PMAA are a wide impedance bandwidth of 87.3% (1 GHz to 2.55 GHz), the 3 dB axial-ratio (AR) bandwidth of 92.3% (1.05 GHz to 2.85 GHz) excluding dual notch bands, the total bandwidth of 35% (1.8 GHz to 2.55 GHz), and the maximum gain of 8.24 dBic within the total bandwidth. Moreover, in order to generate dual band-notched characteristics in a circular polarized antenna, a folded PMAA with multiple U radiators and inverted W slots is proposed.

1. INTRODUCTION

The success of smart mobile phones has motivated and enhanced the development of a wide range of wireless technologies, including for example 3G video phones, WiFi, WIMAX, ZigBee, and Bluetooth. For cost effectiveness and space utilization, wideband antennas that can accommodate several different communication systems are in high demand. In particular, antennas with unidirectional radiation patterns of various beam widths are of interest as they may be mounted on walls or vehicles without degrading their electrical characteristics and without affecting the aesthetics of the mounting bodies. Although PMA has a simple and compact antenna structure, it is a good

Received 3 April 2012, Accepted 2 May 2012, Scheduled 2 June 2012

* Corresponding author: Kyoung-Sub Oh (ksfaraday@msn.com).

competitive solution for such a system because of wide impedance bandwidth [1–3]. There are lots of techniques such as a bevelling, a shorting strip, a multiple feeding strip and loaded plate to increase the impedance bandwidth in the PMA [4–6].

On the other hand, many modern wireless communication systems such as radar, navigation, satellite, and mobile applications use the circular polarized (CP) radiation pattern [7]. The attractive advantages of the CP antenna are existed as follows. Firstly, since the CP antennas send and receive in all planes, it is strong for the reflection and absorption of the radio signal. In the multi-path fading channel environment, the CP antenna overcomes out of phase problem which can cause dead-spots, decreased throughput, reduced overall system performance. Additionally, the CP antenna is more resistant to signal degradation due to inclement weather conditions [8, 9].

Conventional CP antenna is achieved by trimming opposite corners of the patch corners [10, 11], inserting the thin slots on patch [12–19], fed by coplanar waveguide [20]. In these cases, due to the narrow 3 dB axial ratio, it is not possible for the practical use. To solve this problem, the design techniques for the wideband CP antenna have been published on this study over a long period of time. Spiral antennas which have essentially frequency-independent radiation and impedance characteristics over bandwidth are the exemplary wideband CP antenna, but they are bulky and required to achieve the proper phase progression between adjacent spiral arms [21]. To design a low-profile and compact size, the stacked configurations [22–29] with a patch element are employed and the bandwidths are less than 30%. The broadband single-patch CP microstrip antennas with dual capacitively coupled feeds are proposed [30–32]. They feature the simple feeding networks that are composed of a Wilkinson power divider and 90° phase shifters; however, impedance bandwidths are around (20 ~ 30)%.

Prior studied CP antennas have the narrowband antenna element with a narrowband or wideband feeding network. It causes the degraded wideband performance due to the limit of the impedance bandwidth. Therefore, in order to improve the enhanced wideband characteristic, it seems to be a worthwhile subject to investigate the wideband antenna elements having a wideband feeding network. Related works are published in [33] and [34], but they derive the simulated results with an ideal feeding network.

To remove the interference with a unwanted frequency band in a wideband linear polarized antenna, it has been recently demonstrated that by inserting a proper resonator [35] or etching a proper slot [36–40] in the radiating element, a frequency notched or rejected band within

a wide operating bandwidth can be obtained. These band-notched operations are achieved in the linear polarization due to the antenna configuration.

In this paper, a pinwheel-shaped wideband CP PMAA with dual band-notched characteristics is proposed. Details of the wideband CP PMAA and its performance such as impedance bandwidth, axial ratio, frequency notched band, and radiation patterns are presented and discussed.

2. ANTENNA CONFIGURATION

The geometry of the proposed PMAA is shown in Fig. 2. It is fabricated on an RF-35 substrate with a dielectric constant of 3.5 and thickness of 0.5 mm. The size of the ground plane is $150 \times 150 \text{ mm}^2$.

2.1. A Wideband Feeding Network

In the bottom layer of the ground plane, the wideband feeding network is formed and composed of a wideband planar balun [41] and commercial hybrid couplers [42]. The wideband planar balun is achieved by a Wilkinson power divider with a wideband 180° phase shifter.

2.2. Geometry of The Proposed PMAA

The proposed antenna is assembled by inserting a pinwheel-shaped folded antenna element into the four vertical PMAs which are fixed on the ground plane. To improve the antenna performance of the previous PMAA [43], the proposed PMAA has the folded structure for a low-profile configuration and a high directivity toward the zenith,

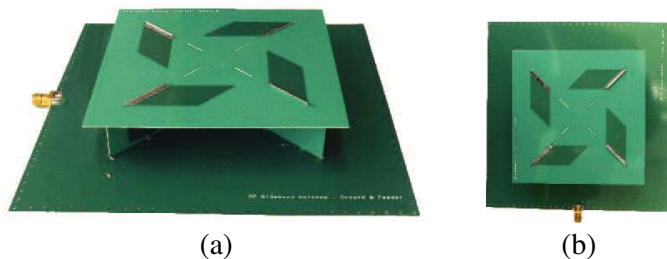


Figure 1. Photograph of the fabricated proposed antenna prototype: (a) Perspective view and (b) top view.

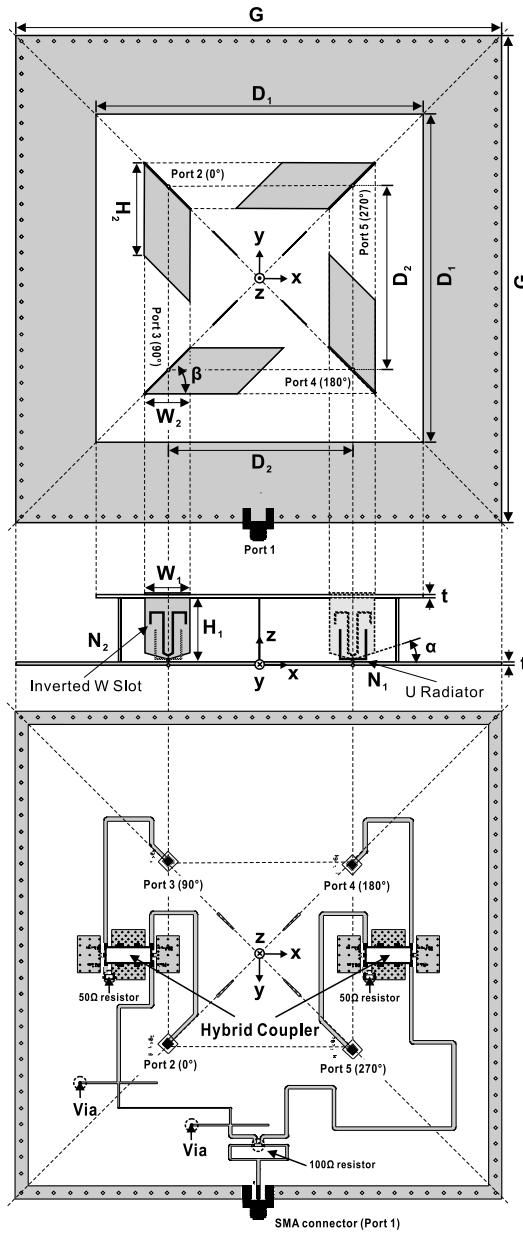


Figure 2. Geometry of the proposed PMAA having the wideband feeding networks which consist of the Wilkinson power divider with a 180° phase shifter and hybrid couplers.

Table 1. Dimension of the proposed antenna configuration.

Part	Parameter	Label	Dimension
Radiator	Vertical PMA Width	W_1	20.0 mm
	Vertical PMA Length	H_1	19.5 mm
	Horizontal PMA Width	W_2	14.1 mm
	Horizontal PMA Length	H_2	28.3 mm
	Antenna Start Beveling	α	12°
	Antenna End Beveling	β	45°
	Dielectric Length	D_1	100 mm
	Substrate Thickness	t	0.5 mm
	Antenna Spacing	D_2	56.5 mm
	Ground Plane Length	G	150 mm
Notch	U Radiator Length	N_1	33.2 mm
	Inverted W Slot Length	N_2	58.6 mm

and a beveling in the proposed PMAs is applied for the wideband characteristic [4].

The proposed PMAA can be divided into the vertical and horizontal antenna elements. The length of the vertical and horizontal elements are $H_1 = 19.5$ mm ($0.13\lambda_0$, where λ_0 is the free-space wavelength at the center of the 3 dB axial ratio bandwidth) and $H_2 = 28.3$ mm ($0.18\lambda_0$), respectively. Their lengths depend on the lower side frequency band, whereas the widths of the antenna element ($W_1 = 20$ mm and $W_2 = 14.1$ mm) decide to the wideband characteristics. Optimized antenna bevels in the vertical and the horizontal antenna element are $\alpha = 12^\circ$ and $\beta = 45^\circ$, respectively.

To generate the good circular polarization, the proposed PMAA has the symmetrical configuration, and it is fed by an equal amplitude and 90° phase difference. From port 1 to port 2, 3, 4, and 5 in Fig. 2, the sequential phases of 0° , 90° , 180° , and 270° are achieved. Table 1 summarizes the dimensions of the proposed PMAA.

3. ANTENNA DESIGN PROCEDURES

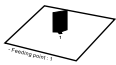
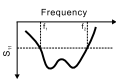
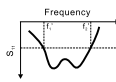
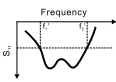
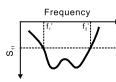
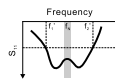
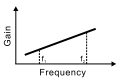
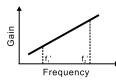
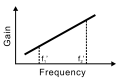
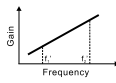
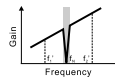
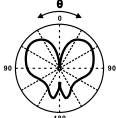
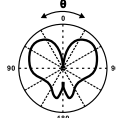
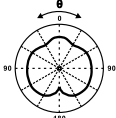
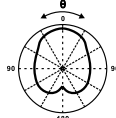
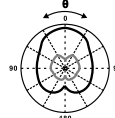
The design procedures of the proposed PMAA consist of five steps as shown in Table 2. Firstly, its design is based on the concept of a PMA with a finite ground plane, which fulfills wide impedance bandwidth

and omni-directional radiation pattern. However, the direction of peak radiation has changed from the xy plane to an angle elevated from that plane. In general, the large the ground plane is, the lower this direction of maximum radiation; as the ground plane approaches infinite size, the radiation pattern approaches a maximum in the xy plane [44].

The second step represents the PMAA which fed by in-phase signals to have the uniform input impedance with respect to the frequency as shown in Table 2. It can achieve higher antenna gain using a impedance matching than a PMA due to the enlarged effective aperture, whereas it also has a null in the zenith direction [45]. However, the PMAA with equal-amplitude power and quadruple phase delay in the operating frequency range can remove the null of a radiation pattern at $\theta = 0^\circ$, and it has the circular polarization in step III [43, 46]. It needs to tune the directions between CP and boresight gain for a high directional antenna characteristic.

To make a high directivity in the zenith direction, the CP PMAA

Table 2. Design procedures of the proposed PMAA.

	Design Steps				
	I	II	III	IV	V
Charac.	PMA	PMAA with a inphase delay	PMAA with a quadruple phase delay	Folded PMAA	Proposed PMAA
Figure					
Return loss					
Gain					
Radiation pattern					
Polar.	Vertical	Vertical	Circular	Circular	Circular

is folded in step IV. In case of the folded antenna, although its input impedance is reduced due to the ground plane, antenna impedance matching is possible using a feeding network for the folded PMAA. From the folded structure, the folded PMAA in step IV can be low-profile, and it has a high directional characteristic.

In order to have a band-notched characteristic in the CP folded PMAA, it is implemented by U radiators [35] or their similar techniques [36] with a symmetric structure. In addition, due to the wideband feeding network, return loss that has nothing to do with a band-stop characteristic is achieved in wideband in step V. From the radiation characteristics such as a radiation pattern and a gain with regard to the frequency, the antenna band-notched functions are verified.

4. RESULTS AND ANALYSIS

4.1. Analysis of the Input Impedance in the PMAA

Four antenna elements which consist of the PMAA are mounted symmetrically on the square ground plane with the antenna spacing (D_2). Those elements are fed by equal-amplitude power and quadruple

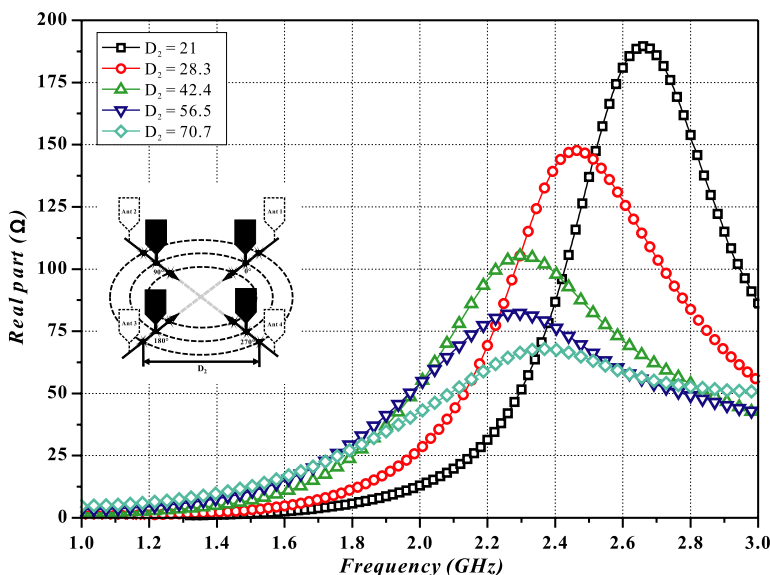


Figure 3. Real parts of input impedance (Z_{in}) with regard to the frequency in the PMAA when the antenna spacing is changed.

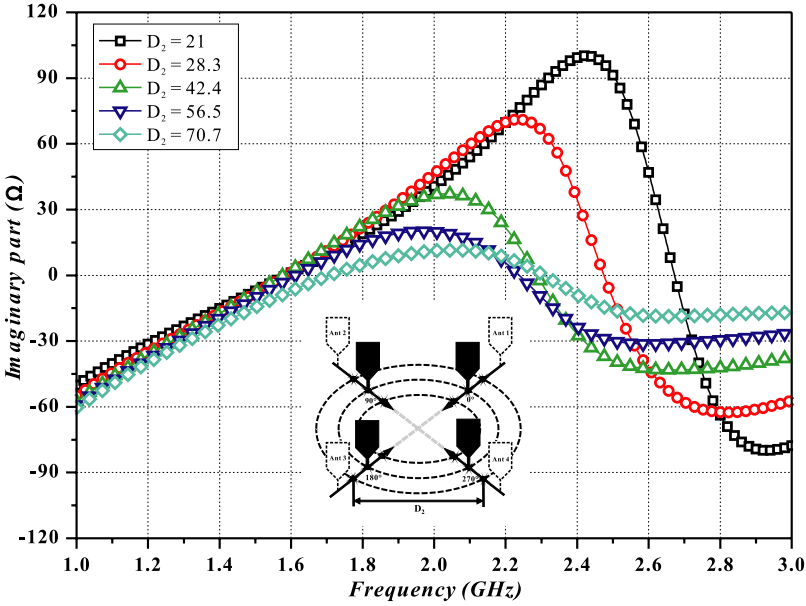


Figure 4. Imaginary parts of input impedance (Z_{in}) with regard to the frequency in the PMAA when the antenna spacing is changed.

phase differences in wideband. Assume voltages and currents at port 2, 3, 4 and 5 are V_1 and I_1 , V_2 and I_2 , V_3 and I_3 , and V_4 and I_4 , respectively.

Since the currents at port 3 and port 5 with regard to port 2 in the antenna input impedance (Z_{in}) are canceled by the equal amplitude and opposite phase, the Z_{in} can be calculated as follows:

$$\begin{aligned} \begin{bmatrix} V_1 \\ V_2 \\ V_3 \\ V_4 \end{bmatrix} &= \begin{bmatrix} Z_{11} & Z_{12} & Z_{13} & Z_{14} \\ Z_{21} & Z_{22} & Z_{23} & Z_{24} \\ Z_{31} & Z_{32} & Z_{33} & Z_{34} \\ Z_{41} & Z_{42} & Z_{43} & Z_{44} \end{bmatrix} \begin{bmatrix} I_1 \\ I_2 \\ I_3 \\ I_4 \end{bmatrix} \\ &= \begin{bmatrix} Z_{11} & Z_{12} & Z_{13} & Z_{12} \\ Z_{12} & Z_{11} & Z_{12} & Z_{13} \\ Z_{13} & Z_{12} & Z_{11} & Z_{12} \\ Z_{12} & Z_{13} & Z_{12} & Z_{11} \end{bmatrix} \begin{bmatrix} I_1 \\ jI_1 \\ -I_1 \\ -jI_1 \end{bmatrix}. \end{aligned} \tag{1}$$

$$\begin{aligned} V_1 &= Z_{11}I_1 + Z_{12}I_2 + Z_{13}I_3 + Z_{14}I_4 \\ &= Z_{11}I_1 + jZ_{12}I_1 - Z_{13}I_1 - jZ_{12}I_1 \\ &= (Z_{11} - Z_{13})I_1. \end{aligned} \tag{2}$$

$$Z_{in} = Z_1 = \frac{V_1}{I_1} = Z_{11} - Z_{13}. \tag{3}$$

As shown in Figs. 3 and 4, when the antenna spacing (D_2) is decreased, the Z_{in} is bigger due to the antenna coupling. For wideband impedance matching, the antenna elements must be at least 50 mm apart.

4.2. Notch Characteristics

To generate the dual band-notched characteristics in the proposed PMAA with a circular polarization, multiple U radiators and inverted W slots are inserted in the PMAA, as shown in Fig. 2. The first notch frequency ($f_{n1} \approx 2.03$ GHz) using the multiple U radiators [35] in the proposed PMAA can be predicted accurately using (4).

$$f_{n1} \approx \frac{c}{\sqrt{\varepsilon_{eff}} \cdot \lambda_{g,n1}} \approx \frac{c}{\sqrt{\varepsilon_{eff}} \cdot 2 \cdot N_1}, \quad (4)$$

where c and ε_{eff} are the speed of light and the approximated effective dielectric constant, respectively, and $\lambda_{g,n1}$ is the guided wavelength at the first fundamental notch frequency (f_{n1}). Also, the second notch frequency ($f_{n2} \approx 2.39$ GHz) using the inverted W slots [36] can be approximated by

$$f_{n2} \approx \frac{c}{\lambda_{g,n2}} \approx \frac{c}{2 \cdot N_2}, \quad (5)$$

where $\lambda_{g,n2}$ is the guided wavelength at the second fundamental notch frequency (f_{n2}). According to (4) and (5), the center frequency of the notch band shifts to lower frequencies as N_1 or N_2 increases.

Figure 5 shows the surface current plots of the averaged amplitude at each notch frequency band for the proposed PMAA. The surface

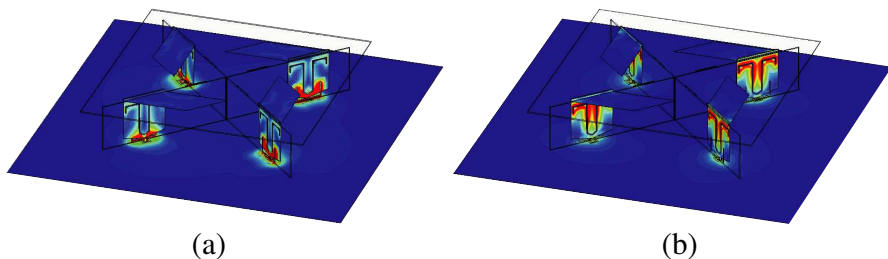


Figure 5. Surface current plots of the averaged amplitude at the notch frequency band in the proposed PMAA: (a) At the first notch frequency (2.03 GHz) and (b) at the second notch frequency (2.39 GHz).

current is concentrated around the top edge of U radiators or Inverted W slots at the notch frequency. This leads to the desired high attenuation near the notch frequency.

4.3. Simulated and Measured Results

To investigate the electrical characteristics of the proposed antenna array, it has been designed and optimized using a 3-D electromagnetic solver (Microwave Studio by CST). The photograph of the fabricated antenna prototype is shown in Fig. 1.

By connecting 50 Ω SMA connectors in the port 1, 2, 3, 4, and 5, the steady amplitude and phase characteristics for the designed feeding network are shown in Fig. 6. Although the amplitude and phase differences between S_{31} and S_{41} or S_{21} and S_{51} are higher at the lower and upper frequency band due to the narrowband characteristics of a Wilkinson divider and hybrid couplers, the wideband CP characteristic has been retained since the performances of the other ports sustain the impedance matching.

Figure 7 shows the simulated and measured results of the proposed

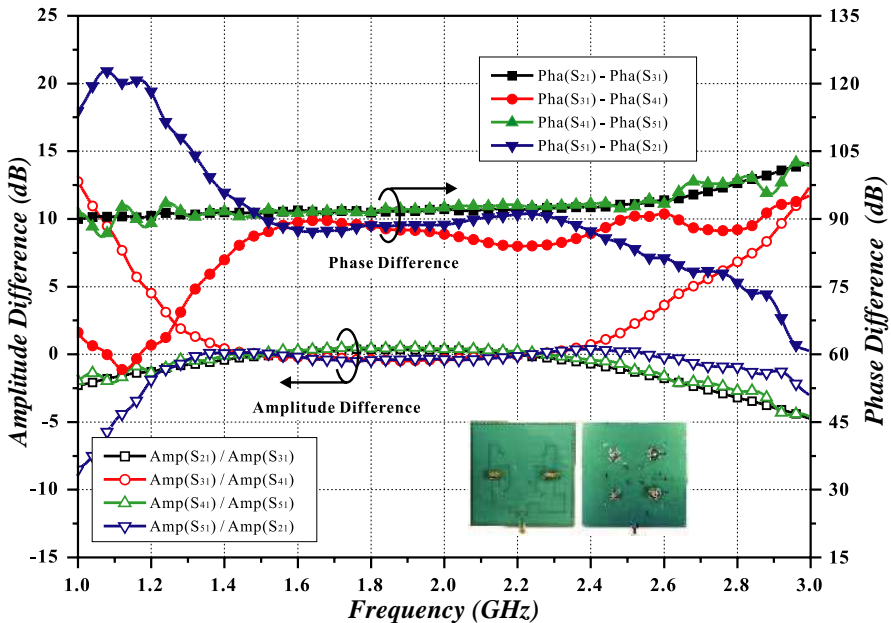


Figure 6. Amplitude and phase differences of the designed feeding networks for the proposed PMAA.

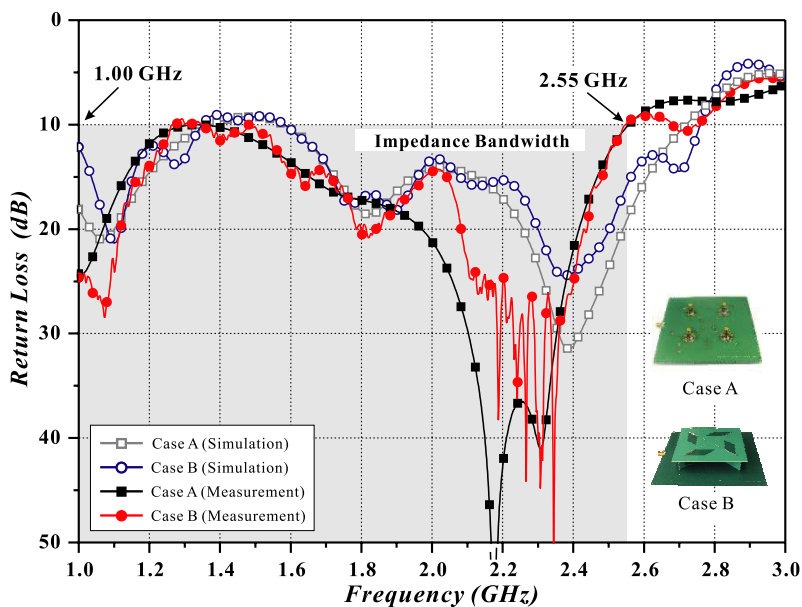


Figure 7. Return loss with regard to the frequency for the proposed PMAA.

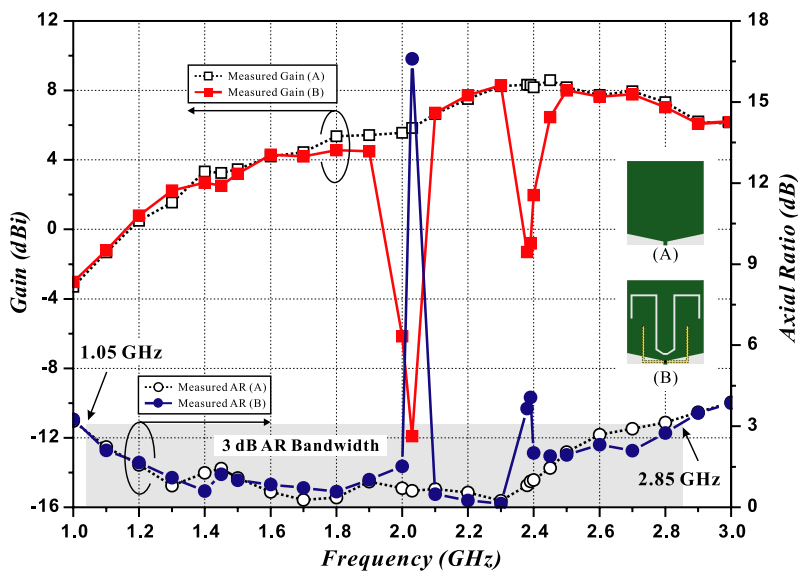


Figure 8. Measured gain and AR bandwidth with regard to the frequency for the proposed PMAA.

PMAA which has an impedance bandwidth of (1.0–2.55) GHz (87.3%). It also shows that return loss in the proposed PMAA (Case B) depends on that of the feeding network with $50\ \Omega$ terminations (Case A).

Figure 8 shows the gain and 3 dB AR with regard to the frequency for the proposed PMAA. The use of pinwheel-shaped folded PMAA structure leads to a maximum gain of 8.24 dBic. The feeding network characteristic causes the low gain in the lower frequency band. From the same figure, 3 dB AR bandwidth is (1.05–2.85) GHz (92.3%), 3 dB gain bandwidth is (1.8–2.9) GHz (49%), and the total antenna bandwidth is (1.8–2.55) GHz (35%). Additionally, due to the dual band-notched characteristics, the antenna radiation gain reductions at the notch frequencies such as 2.03 GHz and 2.39 GHz are more than approximately 10 dB in the direction of maximum gain.

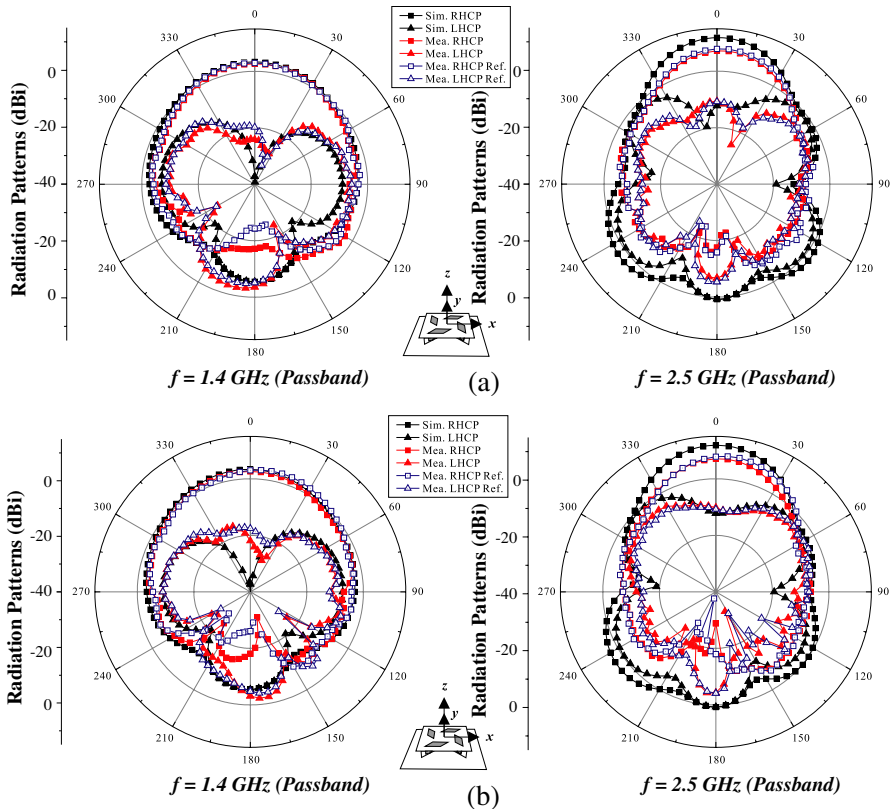


Figure 9. Simulated and measured radiation patterns at 1.4 GHz and 2.5 GHz passband frequency: (a) xz plane, (b) yz plane.

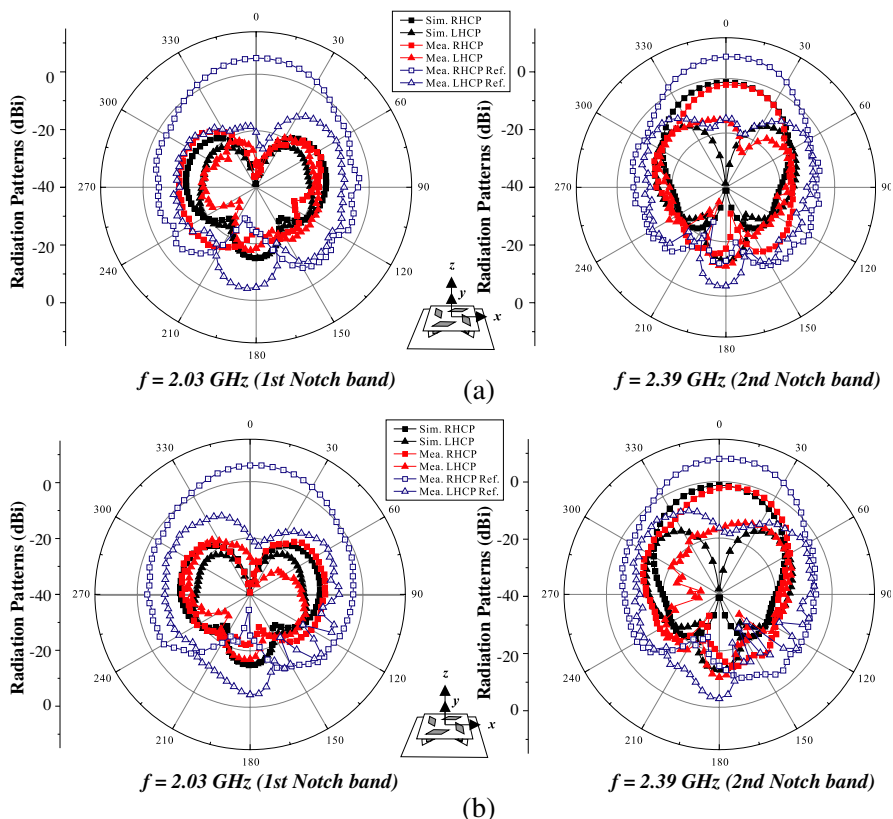


Figure 10. Simulated and measured radiation patterns at 2.03 GHz and 2.39 GHz notch band frequency: (a) xz plane, (b) yz plane.

As shown in Figs. 9 and 10, the simulated and measured radiation characteristics of the proposed PMAA at the different passband and notch band frequencies (1.4, 2.03, 2.39, and 2.5 GHz) are plotted, and measurements agree well with simulations along main beams. The proposed PMAA produces right-hand circular polarization (RHCP) in the wideband frequency. The radiation patterns at the passband frequency are about the same as those of the reference antenna, i.e., the PMAA without inverted W slots or U radiators for band-notching feature. In case of notch band frequencies in Fig. 10, it is noted that the antenna radiation reductions are more than approximately 10 dB in the antenna elevation pattern. Fig. 11 also shows high directivity and attractive axial ratio for the z axis direction.

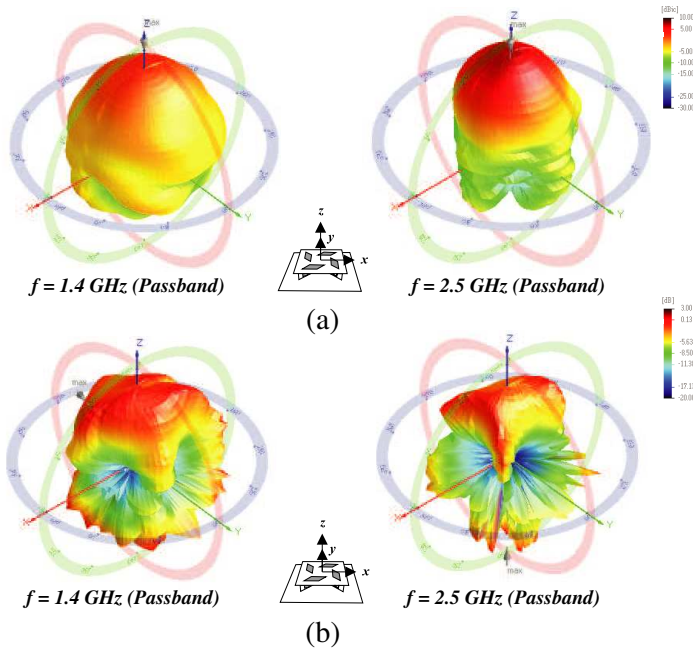


Figure 11. Measured radiation and axial ratio patterns at 1.4 GHz and 2.5 GHz passband frequency: (a) Three-dimensional radiation patterns, (b) axial ratio patterns.

5. CONCLUSION

In this paper, a low-profile, small-sized, pinwheel-shaped wideband PMAA with circular polarized and band-notched characteristics has been proposed. To achieve the high directivity of z axis direction with a wideband bandwidth of 35%, folded antenna array has been implemented. Also, wideband circular polarized antennas with dual band-notched characteristics can be obtained by etching the inverted W slots in the antenna elements and inserting U radiators on the backside of the antenna elements. Due to favorable antenna performance, the proposed PMAA can be useful for many modern wireless communication systems that require wideband circularly polarized radiation patterns and a high directivity.

ACKNOWLEDGMENT

The authors would like to gratefully acknowledge the technical support by Korea Testing Laboratory (KTL).

REFERENCES

1. Agrawall, N. P., G. Kumar, and K. P. Ray, "Wide-band planar monopole antennas," *IEEE Transactions on Antennas and Propagation*, Vol. 46, No. 2, 294–295, Feb. 1998.
2. Ni, W., N. Nakajima, and S. Zhang, "A broadband compact folded monopole antenna for WLAN/WiMAX communication applications," *Journal of Electromagnetic Waves and Applications*, Vol. 24, No. 7, 921–930, 2010.
3. Liu, W.-C., P.-W. Chen, and C.-C. Liu, "Triple-band planar monopole antenna for DMB/WLAN applications," *Journal of Electromagnetic Waves and Applications*, Vol. 24, No. 5–6, 653–661, 2010.
4. Ammann, M. J. and Z. N. Chen, "Wideband monopole antennas for multiband wireless systems," *IEEE Antennas Propagation Magazine*, Vol. 45, No. 2, 146–150, Apr. 2003.
5. Wong, K.-L., C.-H. Wu, and S.-W. Su, "Ultrawide-band square planar metal-plate monopole antenna with a trident-shaped feeding strip," *IEEE Transactions on Antennas and Propagation*, Vol. 53, No. 4, 1262–1269, Apr. 2005.
6. Mazinani, S. M. and H. R. Hassani, "A novel omnidirectional broadband planar monopole antenna with various loading plate shapes," *Progress In Electromagnetics Research*, Vol. 97, 241–257, 2009.
7. Expósito-Domínguez, G., J. M. Fernández-González, P. Padilla, and M. Sierra-Castañer, "Dual circular polarized steering antenna for satellite communications in X band," *Progress In Electromagnetics Research*, Vol. 122, 61–76, 2012.
8. Sichak, W. and S. Milazzo, "Antennas for circular polarization," *Proceedings of the IRE*, Vol. 36, No. 8, 997–1001, Aug. 1948.
9. Toh, B. Y., R. Cahill, and V. F. Fusco, "Understanding and measuring circular polarization," *IEEE Transaction on Education*, Vol. 46, No. 3, 313–318, 2003.
10. Sharma, P. C. and K. C. Gupta., "Analysis and optimized design of single feed circularly polarized microstrip antennas," *IEEE Transactions on Antennas and Propagation*, Vol. 31, No. 6, 949–955, Nov. 1983.
11. Yang, S. L. S., K. F. Lee, and A. A. Kishk, "Design and study of wideband single feed circularly polarized microstrip antennas," *Progress In Electromagnetics Research*, Vol. 80, 45–61, 2008.
12. Wong, K.-L. and J.-Y. Wu., "Single-feed small circularly polarized square microstrip antenna," *Electronics Letters*, Vol. 33, No. 22,

- 1833–1834, Oct. 1997.
13. Kasabegoudar, V. G. and K. J. Vinoy, “A broadband suspended microstrip antenna for circular polarization,” *Progress In Electromagnetics Research*, Vol. 90, 353–368, 2009.
 14. Chen, J., G. Fu, G.-D. Wu, and S.-X. Gong, “A novel broadband circularly polarized irregular slot antenna,” *Journal of Electromagnetic Waves and Applications*, Vol. 24, No. 2–3, 413–421, 2010.
 15. Joseph, R. and T. Fukusako, “Bandwidth enhancement of circularly polarized square slot antenna,” *Progress In Electromagnetics Research B*, Vol. 29, 233–250, 2011.
 16. Sze, J.-Y. and S.-P. Pan, “Design of broadband circularly polarized square slot antenna with a compact size,” *Progress In Electromagnetics Research*, Vol. 120, 513–533, 2011.
 17. Joseph, R. and T. Fukusako, “Circularly polarized broadband antenna with circular slot on circular ground plane,” *Progress In Electromagnetics Research C*, Vol. 26, 205–217, 2012.
 18. Roy, J. S. and M. Thomas, “Design of a circularly polarized microstrip antenna for WLAN,” *Progress In Electromagnetics Research M*, Vol. 3, 79–90, 2008.
 19. Rezaeieh, S. A. and M. Kartal, “A new triple band circularly polarized square slot antenna design with crooked T and F-shape strips for wireless applications,” *Progress In Electromagnetics Research*, Vol. 121, 1–18, 2011.
 20. Matsuzawa, S. and K. Ito., “Circularly polarized printed antenna fed by coplanar waveguide,” *Electronics Letters*, Vol. 32, No. 22, 2035–2036, Oct. 1996.
 21. Dyson, J. D. and P. E. Mayes, “New circularly-polarized frequency-independent antennas with conical beam or omnidirectional patterns,” *IRE Transactions on Antennas and Propagation*, Vol. 9, No. 4, 334–342, Jul. 1961.
 22. Lau, K. L. and K. M. Luk, “A wideband circularly polarized conical-beam patch antenna,” *IEEE Transactions on Antennas and Propagation*, Vol. 54, No. 5, 1591–1594, May 2006.
 23. Chen, X., G. Fu, S. X. Gong, Y. L. Yan, and J. Chen, “Parametric studies on the circularly polarized stacked annular-ring microstrip antenna,” *Progress In Electromagnetics Research C*, Vol. 12, 65–77, 2010.
 24. Du, S., Q.-X. Chu, and W. Liao, “Dual-band circularly polarized stacked square microstrip antenna with small frequency ratio,” *Journal of Electromagnetic Waves and Applications*, Vol. 24,

- No. 11–12, 1599–1608, 2010.
25. Lin, C., F.-S. Zhang, Y. Zhu, and F. Zhang, “A novel three-fed microstrip antenna for circular polarization application,” *Journal of Electromagnetic Waves and Applications*, Vol. 24, No. 11–12, 1511–1520, 2010.
 26. Sun, L., Y.-H. Huang, J.-Y. Li, and Q.-Z. Liu, “A wideband circularly polarized candy-like patch antenna,” *Journal of Electromagnetic Waves and Applications*, Vol. 25, No. 8–9, 1113–1121, 2011.
 27. Chung, K. L., “A wideband circularly polarized H-shaped patch antenna,” *IEEE Transactions on Antennas and Propagation*, Vol. 58, No. 10, 3379–3383, Oct. 2010.
 28. Liu, J. C. and B. H. Zeng, “A dual-mode aperature-coupled stack antenna for WLAN dual-band and circular polarization applications,” *Progress In Electromagnetics Research C*, Vol. 17, 193–202, 2010.
 29. Lau, P.-Y., K. K.-O. Yung, and E. K.-N. Yung, “A low-cost printed CP patch antenna for RFID smart bookshelf in library,” *IEEE Transactions on Industrial Electronics*, Vol. 57, No. 5, 1583–1589, May 2010.
 30. Wong, K.-L. and T.-W. Chiou, “Broad-band single-patch circularly polarized microstrip antenna with dual capacitively coupled feeds,” *IEEE Transactions on Antennas and Propagation*, Vol. 49, No. 1, 41–44, Jan. 2001.
 31. Sun, L., B.-H. Sun, J.-Y. Li, Y.-H. Huang, and Q.-Z. Liu, “Reconfigurable dual circularly polarized microstrip antenna without orthogonal feeding network,” *Journal of Electromagnetic Waves and Applications*, Vol. 25, No. 10, 1352–1359, 2011.
 32. Wang, Y. Z., D. L. Su, and Y. X. Xiao, “Broadband circularly polarized square microstrip antenna,” *7th International Symposium on ISAPE*, 1–4, Oct. 2006.
 33. Zhong, L. L., J. H. Qiu, N. Zhang, and B. Sun, “Analysis and design of novel directional ultra wide-band antennas,” *International Conference on Microwave and Millimeter Wave Technology*, 1658–1661, Apr. 2008.
 34. Zhong, L. L. , J. H. Qiu, N. Zhang, and B. Zhao, “Novel ultrawide-band wide beam circular polarization antenna,” *Asia Pacific Microwave Conference (APMC)*, 1–4, Dec. 2007.
 35. Kim, D.-Z., W.-I. Son, W.-G. Lim, H.-L. Lee, and J.-W. Yu, “Integrated planar monopole antenna with microstrip resonators having band-notched characteristics,” *IEEE Transactions on*

- Antennas and propagation*, Vol. 58, No. 9, 2837–2842, Sep. 2010.
36. Lee, W.-S., D.-Z. Kim, K.-J. Kim, and J.-W. Yu, “Wideband planar monopole antennas with dual band-notched characteristics,” *IEEE Transactions on Microwave Theory and Techniques*, Vol. 54, No. 6, 2800–2806, Jun. 2006.
 37. Zhou, H. J., Q. Z. Liu, Y. Z. Yin, and W. B. Wei, “Study of the band-notch function for swallow-tailed planar monopole antennas,” *Progress In Electromagnetics Research*, Vol. 77, 55–65, 2007.
 38. Li, C.-M and L.-H. Ye, “Improved dual band-notched UWB slot antenna with controllable notched bandwidths,” *Progress In Electromagnetics Research*, Vol. 115, 477–493, 2011.
 39. Hu, Y.-S., M. Li, G.-P. Gao, J.-S. Zhang, and M.-K. Yang, “A double-printed trapezoidal patch dipole antenna for UWB applications with band-notched characteristic,” *Progress In Electromagnetics Research*, Vol. 103, 259–269, 2010.
 40. Zhou, D., S.-C. S. Gao, F. Zhu, R. A. Abd-Alhameed, and J. D. Xu, “A simple and compact planar ultra wide-band antenna with single or dual band-notched characteristics,” *Progress In Electromagnetics Research*, Vol. 123, 47–65, 2012.
 41. Zhang, Z.-Y., Y.-X. Guo, L. C. Ong, and M. Y. W. Chia, “A new wide-band planar balun on a single-layer PCB,” *IEEE Microwave and Wireless Components Letters*, Vol. 15, No. 6, 416–418, Jun. 2005.
 42. LTCC hybrid coupler, “RCP1850S03N,” RN2 Technologies co., Ltd.
 43. Lee, W. S., S. Y. Cha, K. S. Oh, and J. W. Yu, “Wideband circularly polarized planar monopole antenna array,” *Electronics Letters*, Vol. 47, No. 25, 1358–1360, Dec. 2011.
 44. Bahl, I. J. and S. S. Stuchly, “Effect of finite size of ground plane on the impedance of a monopole immersed in a lossy medium,” *Electronics Letters*, Vol. 15, No. 22, 728–729, Oct. 1979.
 45. Kawakami, H., G. Sato, and R. Wakabayashi, “Research on circularly polarized conical-beam antennas,” *IEEE Antennas and Propagation Magazine*, Vol. 39, No. 3, 27–39, Oct. 1997.
 46. Khoo, K.-W., Y.-X. Guo, and C. O. Ling, “Wideband circularly polarized dielectric resonator antenna,” *IEEE Transactions on Antennas and Propagation*, Vol. 55, No. 7, 1929–1932, Jul. 2007.